Research Paper

Menthol evokes Ca^{2+} signals and induces oxidative stress independently of the presence of TRPM8 (menthol) receptor in cancer cells

Mustafa Nazıroğlu[a,b], Walter Blum[c], Katalin Jósvay[d], Bilal Çiğ[b], Thomas Henzi[c], Zoltán Oláh[e,f], Csaba Vizler[d], Beat Schwaller[c], László Pecze[c,*]

[a] Neuroscience Research Center, Suleyman Demirel University, Isparta, Turkey
[b] Department of Biophysics, Faculty of Mediicine, Suleyman Demirel University, Isparta, Turkey
[c] Anatomy, Department of Medicine, University of Fribourg, Route Albert-Gockel 1, Fribourg, Switzerland
[d] Institute of Biochemistry, Biological Research Center of the Hungarian Academy of Sciences, Szeged, Hungary
[e] Institute of Chemistry, Faculty of Materials Science and Engineering, University of Miskolc, Miskolc-Egyetemváros, Hungary
[f] Acheuron Ltd., Szeged, Hungary

ABSTRACT

Menthol is a naturally occurring monoterpene alcohol possessing remarkable biological properties including antipruritic, analgesic, antiseptic, anti-inflammatory and cooling effects. Here, we examined the menthol-evoked Ca^{2+} signals in breast and prostate cancer cell lines. The effect of menthol (50–500 μM) was predicted to be mediated by the transient receptor potential ion channel melastatin subtype 8 (TRPM8). However, the intensity of menthol-evoked Ca^{2+} signals did not correlate with the expression levels of TRPM8 in breast and prostate cancer cells indicating a TRPM8-independent signaling pathway. Menthol-evoked Ca^{2+} signals were analyzed in detail in Du 145 prostate cancer cells, as well as in CRISPR/Cas9 TRPM8-knockout Du 145 cells. Menthol (500 μM) induced Ca^{2+} oscillations in both cell lines, thus independent of TRPM8, which were however dependent on the production of inositol trisphosphate. Results based on pharmacological tools point to an involvement of the purinergic pathway in menthol-evoked Ca^{2+} responses. Finally, menthol (50–500 μM) decreased cell viability and induced oxidative stress independently of the presence of TRPM8 channels, despite that temperature-evoked TRPM8-mediated inward currents were significantly decreased in TRPM8-knockout Du 145 cells compared to wild type Du 145 cells.

1. Introduction

Menthol is a naturally occurring organic compound produced synthetically or obtained from *Mentha arvensis*, (cornmint), *Mentha x piperita* (peppermint), but can also be isolated from other mint oils. Menthol is one of the most widely used natural products consumed as a spice and as a supplement in cosmetics. Menthol has been used for centuries in traditional medicines [1]. Numerous biological properties have been ascribed to menthol such as antipruritic, analgesic, antiseptic, anti-inflammatory, anesthetic and cooling effects [1–3]. Menthol is an agonist for the transient receptor potential cation channel melastatin 8 (TRPM8) receptor, a member of the transient receptor potential (TRP) cation channel super family. The TRP superfamily channels embrace more than 20 agonist-controlled Ca^{2+}/Na^+ channels. They are found in many organs and fulfill various functions [4]. TRPM8 is often considered as a Ca^{2+} channel, yet TRPM8 channels have low selectivity for Ca^{2+} over Na^+ ions compared to other TRP channel

family members [5]. The ability of menthol to evoke a cold sensation is mediated by the cold-sensitive TRPM8 receptors. TRPM8 was initially identified and cloned by screening a prostate-specific subtracted cDNA library showing that TRPM8 was expressed at higher levels in prostate cancer tissue than in normal prostate tissue [6] and was furthermore observed in various other tumors [7]. Overexpression of TRPM8 was reported to be associated with poor prognosis in bladder carcinomas [8] and pancreatic adenocarcinomas [9]. Nevertheless, the precise role of TRPM8 channel in tumor progression remains still unclear. Immunofluorescence experiments revealed expression of TRPM8 protein in the ER ($TRPM8_{ER}$) and the plasma membrane ($TRPM8_{PM}$) in androgen-responsive LNCaP prostate cancer cells [10]. TRPM8 channels are also expressed in sensory neurons and found to play an important role in cold sensation [11].

Calcium ions (Ca^{2+}), acting as signaling molecules, are widely recognized to play a fundamental role in the regulation of various biological processes, e.g. metabolism, proliferation, secretion, and

---

fertilization among others [12]. Many cellular activities carried out in cytosolic and mitochondrial compartments are driven in a Ca^{2+}-dependent manner. Therefore, each cell possesses sophisticated mechanisms for the precise regulation of cytoplasmic ($[Ca^{2+}]_{cyt}$), endoplasmic reticulum luminal ($[Ca^{2+}]_{ER}$) and mitochondrial matrix ($[Ca^{2+}]_{mit}$) Ca^{2+} concentrations. Although cancer cells may accumulate a vast number of mutations and are characterized by having aberrant chromosomes (size and numbers), the Ca^{2+}-regulating toolkit remains active and is able to produce highly organized Ca^{2+} signals including intracellular Ca^{2+} oscillations and moreover intercellular Ca^{2+} waves between adjacent cancer cells. Since Ca^{2+} regulates the cell cycle at several stages, Ca^{2+} signaling is importantly involved in cell-fate determination (quiescent state, proliferation or cell death). Mitogenic compounds such as platelet-derived growth factor, vasopressin, prostaglandin, bombesin or EGF evoke Ca^{2+} transients and also induce inositol trisphosphate ($InsP_3$) production [13,14]. Menthol also induces an increase in $[Ca^{2+}]_{cyt}$ in breast and prostate cell lines, but the published studies presented only the average of evoked $[Ca^{2+}]_{cyt}$ signals in the entire cell population [15,16]. This method blurs the spatiotemporal character of individual intracellular Ca^{2+} signals, which is essential to understand how TRP channel-mediated stimuli influence the cell behavior at the single cell level. At a single cell level intracellular Ca^{2+} oscillations were reported in prostate and breast cancer cells [17,18].

The activation of TRP channels was found to cause a Ca^{2+} accumulation in mitochondria that leads to excessive production of reactive oxygen species (ROS) [19,20]. Epidermal TRPM8 controls the mitochondrial Ca^{2+} concentration and superoxide synthesis in keratinocytes in a cold-dependent manner [21]. ROS and mitochondria also play an important role in apoptosis induction. Cytochrome *c* release from mitochondria triggers caspase activation and finally apoptosis [22]. Ca^{2+} entry and the extent of apoptosis in breast cancer cells is reduced by antioxidant treatments via inhibition of TRP cation channels [23,24], although the precise role of TRPM8 in these processes has not been clarified yet, neither in prostate nor in breast cancer cells. Oil extracts from leaves of *Mentha piperita* show anti-inflammatory and antioxidant activities [25] and induce significant cytotoxicity in human lung carcinoma, leukemia and gastric cancer cell lines [25]. However, in culture medium with reduced serum concentrations, Du 145 prostate cancer cells show a modest, yet significant increase in proliferation induced by menthol [26].

In this study, spatiotemporal recordings of cytoplasmic Ca^{2+} concentrations in various cell lines were collected and analyzed. Since the intensity of the menthol-evoked Ca^{2+} signals was inversely related to the expression levels of TRPM8 in prostate cancer cell lines, we consider it highly unlikely that TRPM8 mediates the effect. To clarify the issue we generated a TRPM8 knockout prostate cancer cell line using the CRISPR/Cas9 method.

2. Materials and methods

2.1. Reagents

L-menthol was purchased from Sigma-Aldrich and dissolved in ethanol (100%) at 1 M concentration. The compound was further diluted with buffer solution used for Ca^{2+} imaging experiments that contained (in mM): NaCl 138, Na_2PO_4 8, $CaCl_2$ 2, $MgCl_2$ 0.5, KCl 2.7, KH_2PO_4 1.6; pH 7.4. In the low Ca^{2+} solution, $CaCl_2$ was replaced with 10 mM EGTA. The final concentration of the solvents were < 0.1% in all experimental solutions. At these concentrations the solvents did not affect/modify the evoked Ca^{2+} responses in control experiments (data not shown). N-(p-amylcinnamoyl)-anthranilic acid (ACA), N-methyl-D glutamine (NMDG), apyrase, AMTB-hydrate (AMTB), suramin, N-acetyl-Asp-Glu-Val-Asp-7-amino-4-methylcoumarin (ACDEVD-AMC), penicillin-streptomycin and dimethyl sulfoxide (DMSO) were purchased from Sigma (St. Louis, MO, USA). Dihydrorhodamine-123 (DHR-123)

was from Molecular Probes (Eugene, OR, USA). N-acetyl-Leu-Glu-His-Asp-7-amino-4-methylcoumarin (AC-LEHD-AMC) was purchased from Bachem (Bubendorf, Switzerland). Icilin, Capsazepine (CapZ) and BCTC were obtained from Tocris Bioscience (Bristol, UK). All reagents were of analytical grade.

2.2. Plasmids and cell lines

The plasmid encoding the full-length human TRPM8 tagged with Myc-DDK was purchased from Origene (#RC220615). In order to get an untagged TRPM8 cDNA driven by the metallothionein gene promoter, *Xho*I and *Mlu*I restriction endonuclease sites were incorporated into the TRPM8 PCR fragment by amplification using specifically designed primer pairs. After cutting the PCR fragment with these enzymes, the size-separated cDNA insert was ligated into the pMTH plasmid containing compatible *Xho*I and *Mlu*I sites [27]. In order to generate a GFP-tagged version of TRPM8, TRPM8 cDNA was amplified with gene-specific forward (5′-CGT CAC TCG AGG AAA AGA TGT CCT TTC G-3′) and reverse (5′ TTA TTT GAT TTT ATT AGC AAT CTC TTT CAG AAG AC-3′) primers. The amplified fragment was cloned into the *Xho*I and *Sma*I sites of pEGFP-C3 plasmid (Clontech). The plasmid encoding $InsP_3$ 5-phosphatase (pIRES-InsP3-5P-GFP) was a kind gift from Christophe Erneux, IRIBHM, Bruxelles [28]. The DNA sequence encoding InsP3-5P was cloned into the *Eco*RI site of pMSCV-IRES-Blue Fluorescent Protein (BFP) plasmid (gift from Dario Vignali, Addgene #52115) to generate the pInsP3-5P-IRES-BlueFP construct.

Human prostate (PC-3, LNCaP, Du 145) and breast (MCF7, BT-474, MDA-MB-231) cancer cell lines, as well as human embryonic kidney cells (HEK-293) were purchased from ATCC (Manassas, VA, USA). Cells were maintained in DMEM containing 10% fetal calf serum and 1% antibiotics (penicillin and streptomycin) at 37 °C in a humidified atmosphere at 5% CO_2.

2.3. Detection of TRPM8 transcripts

RNA isolation from cell lines was performed with TRIzol reagent (Invitrogen, Carlsbad, CA) according to the manufacturer's instructions. Total RNA (600 ng) was reverse-transcribed with the RevertAid™ H Minus First Strand cDNA Synthesis Kit (Fermentas). RT-reaction products (5% of the total RT-reaction volume) were used as templates for the PCR: 95 °C denaturing for 30 s, 60 °C annealing for 30 s, and 72 °C extension time for 40 s, using Taq DNA polymerase (Fermentas). The *TRPM8* transcripts of prostate and breast carcinoma cell lines were detected with specific primer pairs: 5′-CAA GTT TGT CCG CCT CTT TC-3′ (exon 8) and 5′-ACC GCC AGC TCC AGA CAG TT-3′ (exon 10) producing a 579 bp fragment (40 cycles). GAPDH was used as a positive control (20 cycles) with the following primer pairs: 5′-GGT GGT CTC CTC TGA CTT CAA CA-3′ (exon 7) and 5′-GTT GCT GTA GCC AAA TTC GTT GT-3′ (exon 8) producing a 127 bp fragment. The RT-PCR profiling of *TRPM*8-specific mRNA species, either from human prostate or breast carcinoma cell lines were carried out with three independent total RNA samples. PCR products were size separated on agarose gels and visualized with SYBRGreen staining.

2.4. Western blot analysis

The protocol of the Western blot analysis is described in detail elsewhere [29]. Briefly, protein extracts (50 μg) were loaded on 10% SDS polyacrylamide gels. After protein transfer the PVDF membranes were cut at the size of approximately 40 kDa. Antibodies used and their dilutions were: anti-TRPM8 (1:200; rabbit polyclonal, Alomone Labs #ACC-049) and anti-GAPDH (1:10,000, rabbit polyclonal, Sigma Aldrich, # SAB2100894) and anti-rabbit-HRP (1:10,000; goat secondary, Sigma-Aldrich, #A5420). The specificity of the TRPM8 antibody was verified both by the authors [29] and by other researchers [30].

2.5. Ca^{2+} imaging

Cells grown on collagen-coated glass bottom 35 mm dishes (MatTek Corp., Ashland, MA) were loaded with the cell permeable acetoxymethyl (AM)-ester form of the indicator dye. Fluo-4-AM (1 µM; Life Technologies, Grand Island, NY) was used for monitoring changes in $[Ca^{2+}]_{cyt}$ diluted in cell culture media for 20 min at room temperature. After loading, cells were washed with buffer solution (DPBS) used for Ca^{2+}-imaging experiments that contained (in mM): NaCl 138, Na_2PO_4 8, $CaCl_2$ 2, $MgCl_2$ 0.5, KCl 2.7, KH_2PO_4 1.6; pH 7.4. We used an inverted confocal microscope DMI6000 integrated to a Leica TCS-SP5 workstation to examine changes in $[Ca^{2+}]_{cyt}$. The following excitation wavelengths were used to illuminate the Ca^{2+} indicators: 488 nm for Fluo-4 and 561 nm for CAR-GECO1. At the confocal microscope, fluorescence emission was recorded at 510–554 nm (Fluo-4) and 584–683 nm (CAR-GECO1). Recordings were performed at 37 ℃ using Tempcontrol 37-2 digital, and a Heating Stage, all from PeCon GmbH (Erbach, Germany). The drugs were added to the abovementioned solutions by pipette and remained in the solution until the end of the experiments. Fluorescence images for $[Ca^{2+}]_{cyt}$ were collected. Circular-shaped regions of interest (ROI) were placed inside the cytoplasmic area of cells. The fluorescence values were calculated after background subtraction (fluorescence intensity of regions without cells). Bleaching correction was carried out, when the baseline was not stable. Each experimental procedure was repeated at least two times with similar results. Only one series of experiments is presented for each figure, but all parallel experiments were used for statistical evaluation. The LAS-AF (Leica, Wetzlar, Germany) and Prism3 (GraphPad Software, Inc., San Diego, CA) software were used for data analysis.

2.6. Statistical evaluation of the magnitude of menthol-evoked Ca^{2+} signals

The relative fluorescent unit (rfu) values were calculated for each cell; fluorescence intensities at each time point (F(t)) were divided by the averaged baseline fluorescence value measured during the non-treatment period (F(0)):

$$rfu(t) = \frac{F(t)}{F(0)}$$

In order to gain insight into evoked Ca^{2+} responses of the entire cell population observed under the microscope, the traces of more than 20 randomly selected cells were averaged:

$$A(t) = \frac{1}{n} \sum_{i=1}^{n} rfu(t)$$

where n is the number of the selected cells. The integral of the Ca^{2+} signal was calculated as

$$\int_{t1}^{t0} (A(t)-1)*dt$$

where t0 is the time of the onset of $[Ca^{2+}]_{cyt}$ increment and t1 is the endpoint of the recording period (the time when the signal usually returns to its baseline value). This integral was approximated using the trapezoidal rule. The unit for the Ca^{2+} integrals is rfu*sec. The values of integrals from at least three independent experiments were collected and were analyzed further by one-way ANOVA. If the ANOVA test indicated a statistically significant difference between the groups (*p < 0.05), the data were further analyzed by Tukey's multiple comparison post hoc test.

2.7. Generation of the Du 145[M8KO] cell line

Du 145 cells were transduced with lentivirus produced as described before [31,32] with lentiCRISPR - EGFP sgRNA 1 (Addgene #51760) and selected with 2 µg/ml of Puromycin for 5 days. The sgRNA plasmids were obtained from Applied Biological Materials Inc. (Richmond, Canada, #K2536601). Cells were transduced with the lentivirus expressing sgRNA for TRPM8 and selected with 500 µg/ml of Geneticin for 1 week. Clones were selected, genomic DNA extracted and the region of interest (TRPM8 exon1 and 2) amplified by PCR (using Kapa High Fidelity Polymerase) using the following primers: TRPM8_FW 5′- ATG TTG CCT AGC CTG GTC TT-3′, TRPM8_RV: 5′- AAG GTG GAT GTG ACG TGG AT – 3′. The correct fragment size was confirmed by agarose gel electrophoresis and sent for sequencing using the primer: TRPM8_FW 5′- ATG TTG CCT AGC CTG GTC TT-3′. One TRPM8-KO cell line clone was selected for further examination showing a frame shift due to a 1-nt insertion in the TRPM8 DNA sequence (Suppl. Fig. S1). Amplification of a TRPM8-containing DNA fragment of 96 bp containing a MwoI restriction site (GCaa_gtg′tgGC) allowed to distinguishing WT from mutated (GCaaagtg′tgGC; 97-bp fragment) TRPM8 alleles. Obviously the mutated sequence is resistant to cleavage by MwoI (Suppl. Fig. S2).

2.8. Cell viability (MTT) assay

To assess menthol's toxic effects on cell viability, we evaluated the mitochondrial activity of living cells by a 3-(4,5-dimethylthiazol-2-yl)-2,5-diphenyltetrazolium bromide (MTT) quantitative colorimetric assay. After treatment with menthol, the cells were washed and incubated with fresh medium containing MTT (0.5 mg/ml) at 37 ℃ for 90 min. Then, the supernatant was discarded and DMSO was added to dissolve the formazan crystals. The absorbance in each well was measured at 650 nm using a microplate reader (Infinite Pro200; Tecan Austria GmbH, Groedig, Austria) [33]. We performed a total of 6 experiments (n=6) for the cell viability assays. The data were presented as percentage relative to the control.

2.9. Assay for apoptosis markers

Apoptosis was evaluated using the APOPercentage Apoptosis Assay (Biocolor, Belfast, Northern Ireland) according to the manufacturer's instructions. In a viable cell, maintaining the asymmetric composition of membrane lipids is an energy-dependent process involving the activity of flipase enzymes. The loss of asymmetry serves as an early indicator of apoptosis. When the membrane of an apoptotic cell loses its asymmetry, the APOPercentage dye is actively transported into cells, staining apoptotic cells red, thus allowing detection of apoptosis by spectrophotometry. Absorbance was measured at 550 nm (Infinite Pro200). The data were presented as fold increase normalized to control. The determinations of caspase-3 and caspase-9 activities were based on a method previously reported [23] with minor modifications. Cleavage of the caspase-3 substrate (AC-DEVD-AMC) and caspase-9 substrate (AC-LEHD-AMC) was measured in a microplate reader (Infinite pro200) with an excitation wavelength of 360 nm and emission at 460 nm. The data were calculated as fluorescence units/mg protein and presented as fold increase normalized to control.

2.10. Intracellular ROS measurement

DHR 123 is a non-fluorescent, non-charged dye that easily penetrates cell membranes. Once inside the cell, DHR 123 gets fluorescent upon oxidation to yield rhodamine 123 (Rh 123), the fluorescence being proportional to ROS generation. The fluorescence intensity of Rh 123 was measured in a microplate reader (Infinite Pro200). Excitation was set at 488 nm and emission at 543 nm [33]. We performed a total of 6 experiments (n=6) for the intracellular ROS assays. The data were presented as fold increase normalized to control.

2.11. Electrophysiology

Whole-cell voltage-clamp recordings were performed in Du 145[WT] (wild type) and Du 145[M8KO] knockout cells at 15–27 ℃ (EPC10 patch-

clamp set, HEKA, Lamprecht, Germany). Resistances of the recording electrodes were adjusted to about 3–7 MΩ by a puller (PC-10 Narishige International Limited, London, UK). We used standard extracellular bath and pipette solutions as described in a previous study [34]. The holding potential for the patch-clamp analyses was set at −60 mV. The voltage-clamp technique was used for the analyses; the current-voltage (I-V) relationships were obtained from voltage ramps from −90 to +60 mV applied over 200 ms. All experiments were performed at room temperature (22 ± 1 °C). Cold exposure of Du 145[WT] and Du145[M8KO] cells was achieved in a slice mini bath chamber with a controller type TC05 (No: 200-100 500 0150, Luigs and Neumann, Ratingen, Germany) as described in a previous study [34]. After gating the channels with cold exposure in Du 145[WT] cells, TRPM8 channels were extracellularly blocked by administration of ACA (0.025 mM) via patch chamber. For the analysis, the maximal current amplitude (pA) in a given Du 145 cell was divided by the cell capacitance (pF), a measure of the cell surface. The results in the patch-clamp experiments are the current density relationships (pA/pF).

2.12. Mitochondrial membrane potential determination

Cells were incubated with 1 μM JC-1 for 15 min at 37 °C as previously described [35]. JC-1 is a lipophilic, cationic dye that selectively enters into mitochondria and reversibly changes color from red to green as the mitochondrial potential decreases. The green signal was measured at an excitation wavelength of 485 nm and an emission wavelength of 535 nm, the red signal at an excitation wavelength of 540 nm and an emission wavelength of 590 nm. Fluorescence values were measured using the microplate reader Infinite Pro200 and the green/red fluorescence intensity ratio was calculated. The data were presented as fold increase normalized to control.

3. Results

3.1. Expression patterns of the thermo-sensitive TRP channel TRPM8 in cancer cell lines

Three prostate (PC-3, LNCaP and Du 145) and three breast (MCF7, BT-474 and MDA-MB-231) carcinoma cell lines were tested for the presence of TRPM8 channel transcripts (Fig. 1A). The *TRPM8* signal was highly variable: a very strong signal was detected in LNCaP cells, intermediate signals in the remaining ones, with the exception of MCF7, where almost no signal was detected. At the protein level, Western blot analysis showed that all cell lines expressed TRPM8 (Fig. 1B). The TRPM8 antibody revealed 130 kDa bands specific for TRPM8 protein in all cell lines including MCF7 cells, despite the very faint PCR signal for a *TRPM8* transcript in these cells.

3.2. Analyses of the menthol-induced changes in $[Ca^{2+}]_{cyt}$ in carcinoma cell lines

Menthol (500 μM) evoked Ca^{2+} oscillations in $[Ca^{2+}]_{cyt}$ and intercellular Ca^{2+} waves in all cell lines, except in LNCaP cells (Fig. 2A-F). Very few (< 1%) of the LNCaP cells showed menthol-evoked single Ca^{2+} transients that never led to oscillations (Fig. 2B). In order to test whether LNCaP cells were able to produce Ca^{2+} oscillations at all, we used the previously used serum re-administration protocol. Serum contains a plethora of growth factors and hormones potentially activating many G protein coupled receptors. Transient serum withdrawal followed by serum re-administration is a well-known mechanism of activating the inositol phospholipid pathway [31,36]. Serum re-administration 24 h after serum deprivation induced long-lasting Ca^{2+} oscillations also in LNCaP cells (Fig. 2G). Comparison of the integrals of the Ca^{2+} response reveled that Du 145 cells produced the strongest and LNCaP cells the weakest Ca^{2+} response (PC-3: 194 ± 28, LNCAP: 1.6 ± 1.1, Du 145: 257 ± 41, MCF7: 217 ± 61, BT 474: 68 ± 13, MDA-
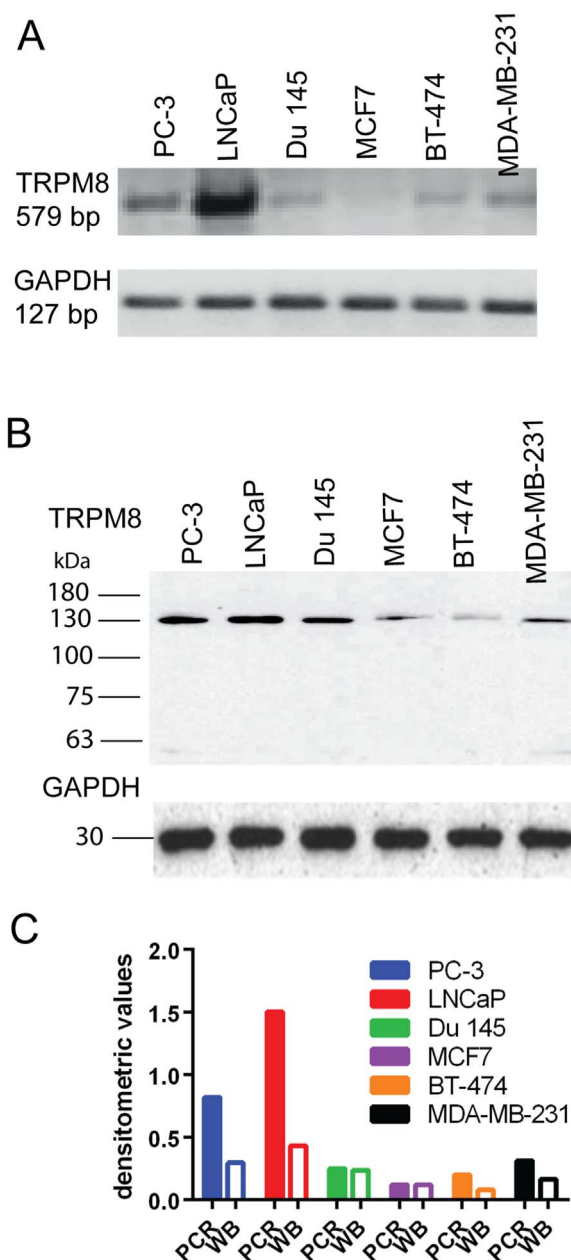
Fig. 1. Detection of TRPM8 transcripts and protein in prostate and breast cancer cell lines. **A)** Signals for *TRPM8* mRNA were found in cell lines derived from prostate cancer-derived (lanes 1–3) and breast cancer-derived (lanes 4–6) cell lines. The normalization with the *GAPDH* housekeeping control allowed to semi-quantitatively assessing the abundance of the different transcripts present in each sample. **B)** Signals for TRPM8 protein were detected in all cell lines; the ones for MCF7 and BT-474 were weaker than for the other cell lines (expected mass: 129 kDa). The GAPDH protein signal was used as a loading control. **C)** Densitometry analysis. The values of TRPM8 expression for mRNA (filled columns) and protein (empty columns) levels were normalized to the values of GAPDH controls.

MB-231: 148 ± 29, all in rfu*sec) (Fig. 2H). The relative fluorescence unit (rfu)*second (sec) values represent the magnitude of the integrals of the evoked Ca^{2+} signals. At a lower menthol concentration (50 μM) the integrals of Ca^{2+} responses were smaller (MCF7; 217 ± 61 vs 41 ± 13 rfu*sec, p < 0.05, Student *t*-test; PC-3 194 ± 28 vs. 31 ± 23 all in rfu*sec, p < 0.05, Student *t*-test), yet this menthol concentration was better suited to investigate intercellular Ca^{2+} waves (Fig. 2I). The waves started from few "initiator" cells and then spread more or less radially in all directions often joining with waves having started from distant "initiator" cells. The Ca^{2+} wave velocity was 9.5 ± 2.5 μm/s for
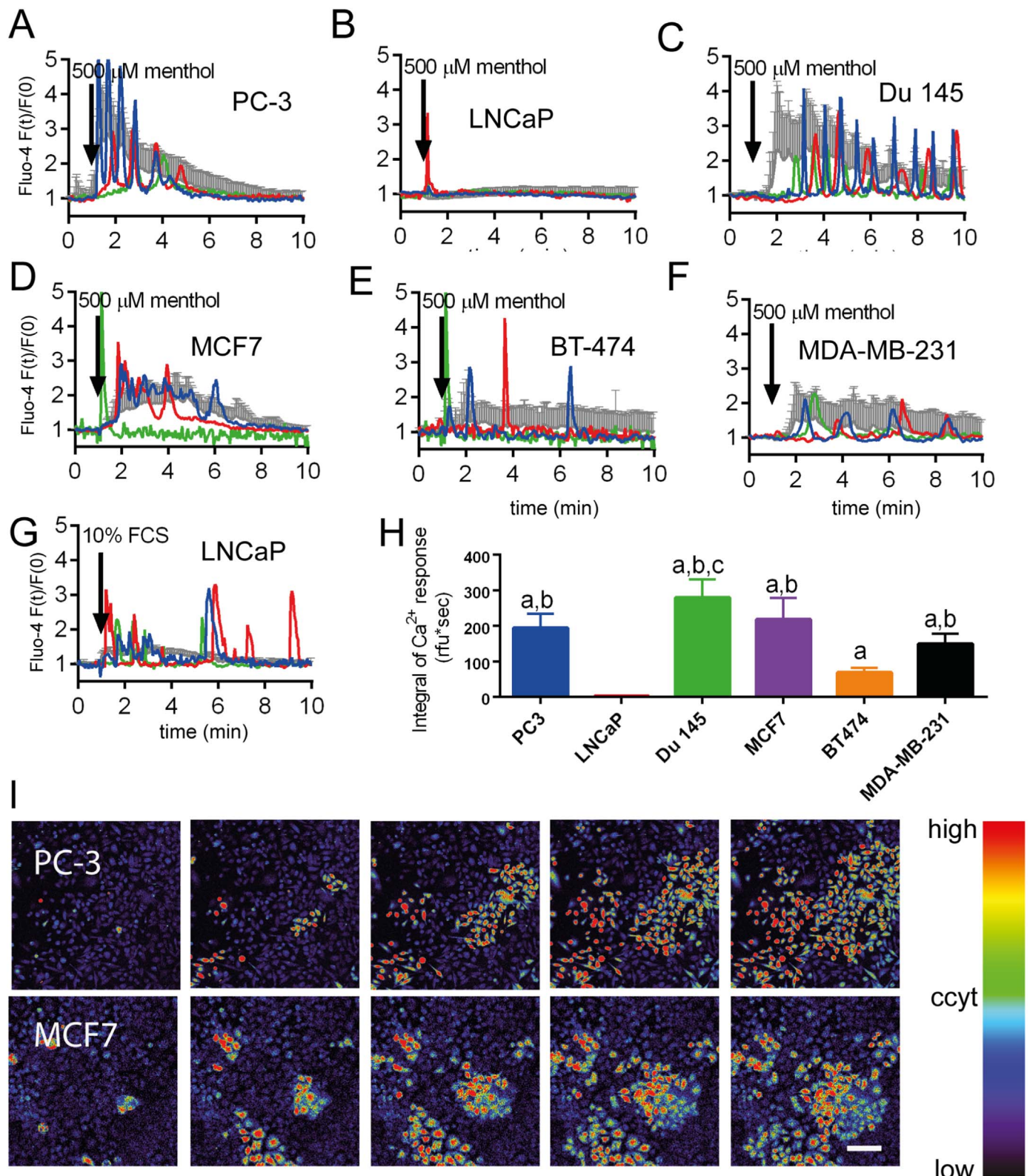
Fig. 2. Menthol-evoked changes in the cytoplasmic free Ca^{2+} concentrations. A)-G) Single-cell (colored traces) and average fluorescence (grey traces) recordings from time-lapse videos show changes in $[Ca^{2+}]_{cyt}$ after menthol administration. Bars represent standard deviations (SD). Experiments were repeated at least two times with similar results. PC-3 (**A**), Du 145 (**C**), MCF7 (**D**) BT-474 (**E**) and MDA-MB-231 (**F**) cells treated with menthol (500 µM) showed Ca^{2+} waves and Ca^{2+} oscillations. Very few (< 1%) LNCaP cells (**B**) responded to menthol with a small single Ca^{2+} transient. **G)** Ca^{2+} signals induced in LNCaP cells by serum re-administration. **H)** Statistical comparison of the integrals of menthol-evoked Ca^{2+} responses. The letters denotes the following **a**- significant difference from LNCaP cells **b**-significant difference from BT-474 cells, **c**-significant differences from MDA-MB-231 cells, $p < 0.05$, One-way ANOVA + Tukey's post-hoc test **I)** Time-lapse image series of Ca^{2+} waves. The acquisition rate was set to 3 s. Blue and red colors depict lower and higher fluorescence intensities, respectively. A Ca^{2+} wave in PC-3 (upper row) and MCF7 cells (lower row) was evoked by administration of 50 µM menthol. Scale bar represents 150 µm. (For interpretation of the references to color in this figure legend, the reader is referred to the web version of this article.)
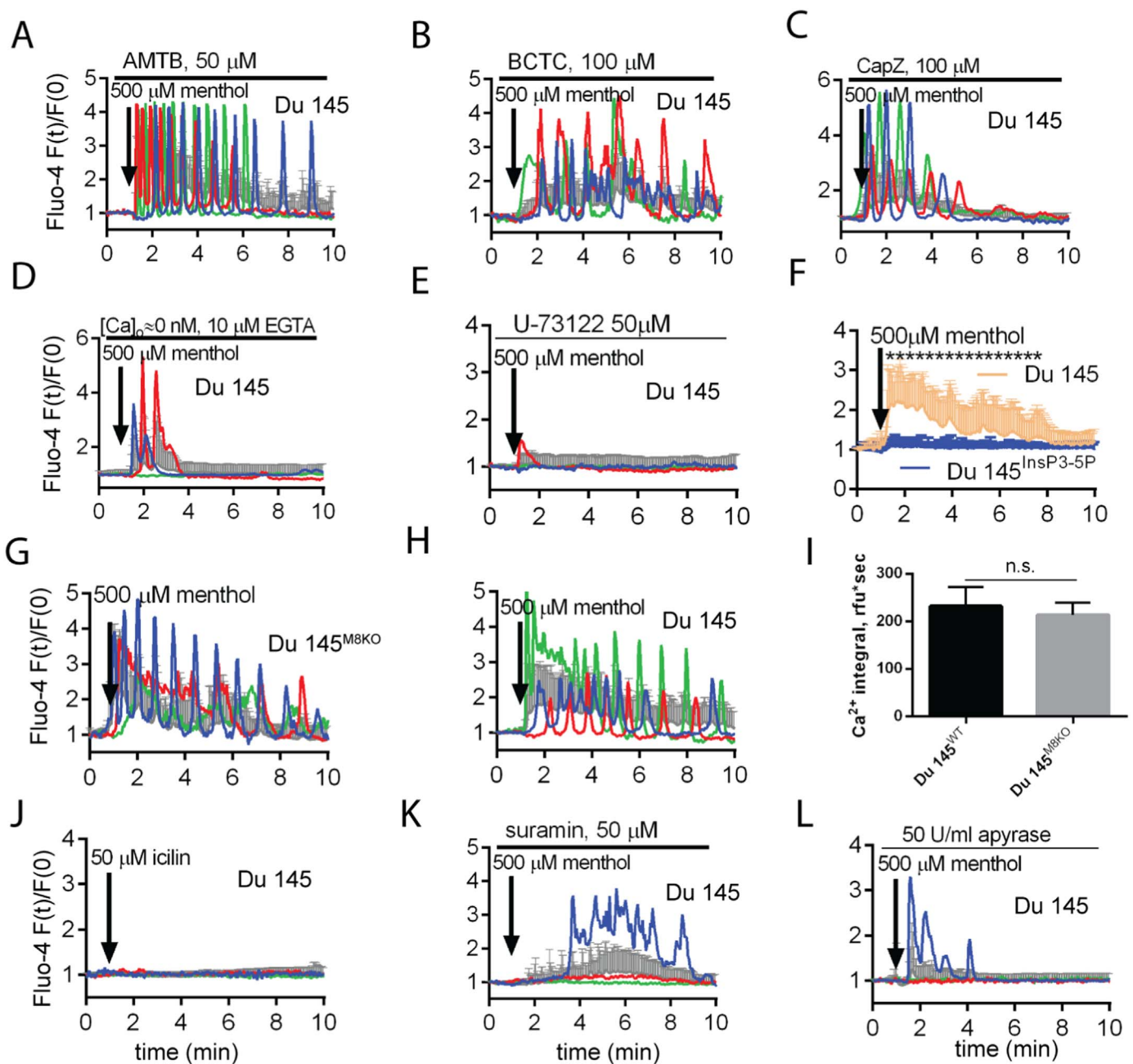
Fig. 3. The effect of different Ca^{2+} signal modulators on menthol-evoked responses. A)- L) Single-cell (colored traces) and average fluorescence (grey traces) recordings from time-lapse videos show changes in $[Ca^{2+}]_{cyt}$. Bars represent standard deviations (SD). Each figure represents the results of one representative experiment out of three with similar results. **A)** ATMB hydrochloride, a TRPM8 blocker administered before menthol had no effect on menthol-evoked Ca^{2+} response **B)** BCTC, a putative TRPM8 blocker, administered before menthol had no effect on menthol-evoked Ca^{2+} responses. **C)** CapZ, an another putative TRPM8 blocker had no effect on menthol-evoked Ca^{2+} responses. **D)** Removing the extracellular Ca^{2+} ions strongly reduced the menthol-evoked responses **E)** Cells pre-treated with 50 μM U-73122 did not show oscillations. **F)** Overexpression of $InsP_3 - 5$-phosphatase hydrolyzing $InsP_3$ with concomitant BFP expression in transfected cells inhibited menthol-induced oscillations compared to the non-transfected cells. Blue and yellow traces represent average fluorescence recordings from cells with or without $InsP_3 - 5$-phosphatase from the same culture dish, respectively. Asterisks represent significant differences, $p < 0.05$, student t-test. **G-H)** A Du 145[M8KO] cell clone responded to menthol (**G**) similar as control Du 145 cells (**H**). **I)** Statistical analysis on the integrals of the evoked Ca^{2+} responses also showed no significant differences (integrals are from 4 consecutive experiments). J) Icilin did not evoke Ca^{2+} oscillations. **K)** Suramin, a non-specific purinergic receptor blocker, strongly reduced the menthol-evoked responses. **L)** The presence of apyrase in the extracellular milieu also strongly reduced the menthol-evoked responses indicative of a role of extracellular ATP release after menthol treatment. (For interpretation of the references to color in this figure legend, the reader is referred to the web version of this article).

PC-3 cells and 12.3 ± 2.5 μm/s for MCF7 cells (Fig. 2I, upper and lower rows, respectively).

3.3. Characterization of menthol-induced changes in $[Ca^{2+}]_{cyt}$ in Du 145 cell lines

Since Du 145 cells showed the most pronounced response to menthol among the examined cancer cell lines, we selected this one for further analysis. ATMB hydrochloride, a specific TRPM8 antagonist [37], administered before menthol (500 μM), had no significant effect on menthol-evoked Ca^{2+} responses (257 ± 41 vs 243 ± 38 rfu*sec, $p > 0.05$, Student t-test) (Fig. 3A). Similarly CapZ (257 ± 41 vs 163 ± 68 rfu*sec, $p > 0.05$, Student t-test) (Fig. 3B) and BCTC (257 ± 41 vs 178 ± 48 rfu*sec, $p > 0.05$, Student t-test) (Fig. 3C), proven TRPV1 inhibitors and putative TRPM8 blockers, administered before menthol had no obvious effect on menthol-evoked Ca^{2+}

responses. These findings suggest that neither TRPM8 nor TRPV1 were involved in the menthol-evoked responses.

Removal of extracellular Ca^{2+} ions by 10 mM EGTA strongly reduced menthol-evoked responses (257 ± 41 vs 40.3 ± 7.8 rfu*sec, p < 0.05, Student t-test) and decreased the percentage of the responding cells from 91 ± 5% to 30 ± 11% (Fig. 3D). Cells pre-treated with 50 μM U-73122, a specific phospholipase C inhibitor didn't show oscillations (257 ± 41 vs 2.5 ± 3 rfu*sec, p < 0.05, Student t-test) (Fig. 3E). Overexpression of InsP$_3$-5-phosphatase, an enzyme hydrolyzing InsP$_3$ and concomitant expression of BFP using the pInsP3-5P-IRES-BFP construct inhibited menthol-induced oscillations in Du 145 cells. BFP was used as a transfection control in order to identify cells overexpressing InsP$_3$-5-phosphatase. Blue and yellow traces represent average fluorescence recordings from cells with or without InsP$_3$-5P from the same culture dish, respectively (Fig. 3F). These finding indicate that InsP$_3$ production and Ca^{2+} transport across the plasma membrane play an essential role in the menthol-evoked responses.

In order to clarify the role of TRPM8 channels in the menthol-evoked Ca^{2+} response, a TRPM8-knockout cell line was generated using the CRISPR/Cas9 technology. A TRPM8 knockout cell clone (representative for several other tested clones) responded to menthol (500 μM) in a similar manner as the parental Du 145 cells (Fig. 3G-H). No statistical differences were observed between the integrals of evoked Ca^{2+} responses (257 ± 41 vs 235 ± 47 rfu*sec, p > 0.05, Student t-test) (Fig. 3I). Moreover, icilin (50 μM), another TRPM8 activator, did not produce significant Ca^{2+} signals in Du 145 cells (257 ± 41 vs 9.2 ± 3.9 rfu*sec, p < 0.05, Student t-test) (Fig. 3J). All together, these findings demonstrate that menthol evokes Ca^{2+} signals independently of TRPM8.

Since in many cases, intracellular Ca^{2+} signals may result in the formation of Ca^{2+} waves in cell ensembles and moreover Ca^{2+} waves are a consequence of released and extracellularly propagating ATP molecules, we examined whether a blockage of this process may inhibit the menthol-evoked responses. ATP molecules acting on purinergic receptors evoke Ca^{2+} responses in many cell lines, also in Du 145 cells [17]. Suramin, a blocker of purinergic receptors strongly reduced menthol-evoked Ca^{2+} responses (257 ± 41 vs 66 ± 38 rfu*sec, p < 0.05, Student t-test) (Fig. 3K). Similarly, the presence of apyrase in the extracellular milieu, an enzyme that catalyzes the hydrolysis of ATP to yield AMP and inorganic phosphate, strongly reduced the menthol-evoked responses (257 ± 41 vs 10.9 ± 6.5 rfu*sec, p < 0.05, Student t-test) (Fig. 3L).

3.4. The effect of ectopically expressed TRPM8 on Ca^{2+} signals

Previously, it was reported that HEK-293 cells also show menthol-evoked Ca^{2+} signals independent of TRPM8 receptor [38] a finding that we confirmed in HEK-293 cells subjected to 500 μM menthol. The characteristics of Ca^{2+} responses were similar to responses observed in PC-3 and MCF7 cells after treatment with 50 μM menthol, also including the generation of Ca^{2+} waves spreading through an area of cells (Fig. 4A). In non-transfected HEK-293 cells the addition of menthol (50 μM) did not evoke a signal, while Ca^{2+} signals were evident in similarly treated HEK-293^{TRPM8} cells indicating that overexpression of TRPM8 lowers the threshold concentration required for menthol-induced Ca^{2+} signals (Fig. 4C, yellow and green curves, respectively). Previous reports had indicated that TRPM8 is present both in the plasma membrane (TRPM8$_{PM}$) and in ER membranes (TRPM8$_{ER}$) [10]. In order to distinguish the role of TRPM8$_{ER}$ and TRPM8$_{PM}$ in the menthol-evoked Ca^{2+} signals, HEK-293^{TRPM8} cells were stimulated with menthol in a Ca^{2+}-free extracellular environment. In the absence of extracellular Ca^{2+} ions the menthol-evoked Ca^{2+} responses were strongly reduced, i.e. nearly eliminated (Fig. 4D). This indicated that TRPM8$_{ER}$ channels have a small (if any) contribution to the menthol-evoked Ca^{2+} signals when compared to the contribution of TRPM8$_{PM}$. We confirmed the ER localization of ectopically expressed TRPM8 in

HEK 293 cells. For this we used GFP-tagged TRPM8 (green) and ER-located mCherry (red). The yellow color on the merged image indicates partial overlap (Fig. 4E).

3.5. Assessing the effect of menthol treatment on the viability and apoptosis of Du 145 and Du 145^{M8KO} cells

Next, we investigated how menthol influences the cell viability of Du 145 cells also in relation to TRPM8 expression. Serial dilutions of menthol were applied to Du 145^{WT} and Du 145^{M8KO} cells. Only at the highest menthol concentration (500 μM) viability was significantly decreased (p < 0.05) in both cell lines indicating that the effect was unlikely mediated by TRPM8. At lower menthol concentrations, cell viability was unaffected in both cell lines. (Fig. 5A). The effects of menthol on the induction of apoptosis were determined in two independent ways: by determination of the loss of the plasma membrane asymmetry and by measuring the increased caspase activities; caspase-3 and caspase-9 (Fig. 5B, C and D, respectively). Data analyses of the two complementary methods resulted in a rather congruent picture. A loss of membrane asymmetry (higher APOP values) and increased activities of caspase-3 and caspase-9 were observed in all menthol-treated groups; the higher the concentration of menthol applied, the higher values in all three assays were observed. In the apoptosis assay Du 145^{WT} cells showed a small but significant increase in their sensitivity to menthol-induced apoptosis compared to Du 145^{M8KO} cells, at all 3 menthol concentrations tested. No significant differences between Du 145^{WT} and Du 145^{M8KO} cells were observed in both caspase activation assays. The results are indicative of a mainly TRPM8-independent involvement of menthol in the activation of the apoptotic pathway, since activation of caspase-3 (intrinsic + extrinsic) and caspase-9 (intrinsic) pathways were in all cases of similar magnitude.

3.6. Effect of menthol treatment on reactive–oxygen species (ROS) production and mitochondrial membrane depolarization

Most Ca^{2+} ions entering the cytoplasm from internal Ca^{2+} stores or from the external side are taken up into mitochondria [36,39]. Subsequently, mitochondrial Ca^{2+} accumulation leads to mitochondrial depolarization, i.e. the mitochondrial membrane potential (Ψ_m) diminishes resulting in an increase in intracellular ROS production and oxidative stress [40]. Mitochondrial membrane depolarization (estimated by the JC-1 assay and reported as a ratio) and ROS production (estimated by the DHR assay) were affected by menthol treatment in a dose-dependent manner in all treatment groups (Fig. 6A and B). Again in most cases, small, but statistically significant differences were found between Du 145^{WT} and Du 145^{M8KO} cells. These results point towards an effect of menthol on mitochondrial activity and oxidative stress, partially mediated by TRPM8.

3.7. Effects of cold on TRPM8 channel currents in Du 145 cells with and without functional TRPM8

To corroborate the importance of cold temperature for the activation of TRPM8 channels, functional channel experiments were carried out using the patch-clamp technique using equipment allowing for controlled bath temperature. When the temperature was decreased from 27 °C to 15 °C, no temperature-dependent currents were seen in Du 145^{M8KO} cells (Fig. 7A). TRPM8 channels in Du 145^{WT} cells were clearly activated by cold exposure starting at around 19 °C (Fig. 7B). Currents induced by cold developed gradually during exposure to the cold and reached amplitudes of larger than −1.95 nA at 15 °C. These currents were reversibly blocked by ACA, a TRPM8 blocker. Replacement of external Na^+ with $NMDG^+$ also blocked the inward currents (Fig. 7B). Current density was significantly (p ≤ 0.001) higher in Du 145^{WT} cells than in Du 145^{M8KO} cells (Fig. 7C). The current density was markedly lower in ACA-treated Du 145^{WT} cells (p ≤ 0.001).
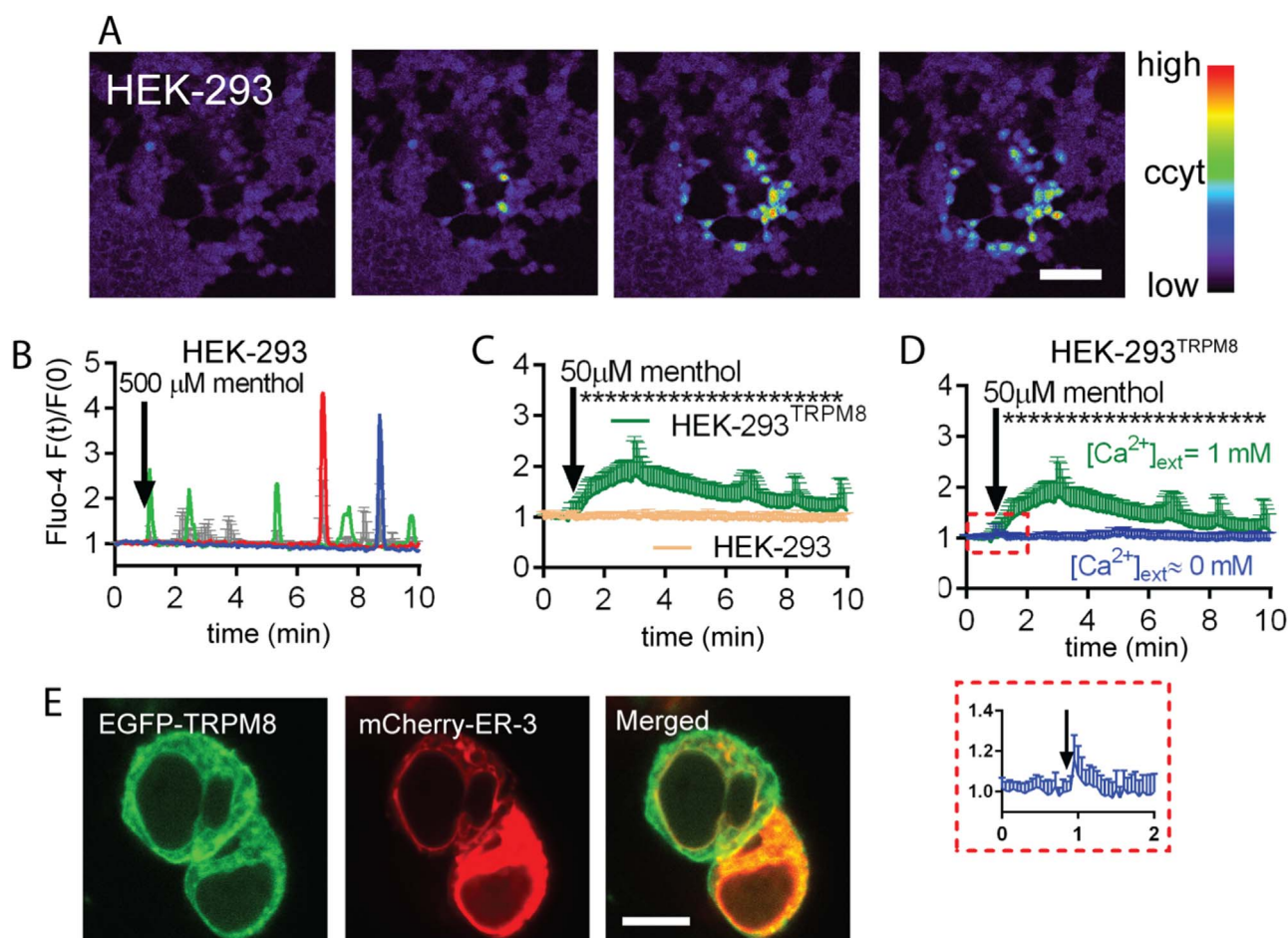
Fig. 4. Menthol-evoked responses in HEK-293 cells. A) Time-lapse image series of Ca^{2+} waves. The acquisition rate was set to 3 s. Blue and red colors depict lower and higher fluorescence intensities, respectively. A Ca^{2+} wave in HEK-293 cells was evoked by administration of 500 μM menthol. Bar represent 100 μm. **B)** Single-cell (colored traces) and average fluorescence (grey traces) recordings from time-lapse videos show changes in $[Ca^{2+}]_{cyt}$. Bars represent standard deviations (SD). A Ca^{2+} response in HEK-293 cells was evoked by administration of 500 μM menthol. **C)** Non-transfected HEK-293 cells didn't respond to 50 μM menthol, but responded, if cells were transfected with a plasmid encoding the human TRPM8 receptor (yellow trace and green traces, respectively). D) Transfected HEK-293 cells showed only very small responses to 50 μM menthol in the absence of extracellular Ca^{2+} ions; see magnification of the traces in absence of extracellular Ca^{2+} in the boxed red area. This indicates that essentially TRPM8$_{PM}$ channels are involved in the Ca^{2+} responses. **C-D)** Traces show average fluorescence values with SD. Asterisks represent significant differences, p < 0.05, Student *t*-test. **E)** EGFP-TRPM8 (green) and mCherry-ER proteins (red) showed partial co-localization (yellow color on the merged image). Bar represent 10 μm. (For interpretation of the references to color in this figure legend, the reader is referred to the web version of this article).

4. Discussion

In line with previous findings on elevated TRPM8 levels in tumor tissue, we demonstrated that also breast cancer- and prostate cancer-derived cell lines expressed transcripts for *TRPM8*. TRPM8 protein was also expressed in all 6 investigated cell lines. All but one (LNCaP) of the investigated cell lines responded to menthol stimulation at either 50 or 500 μM with elevations of $[Ca^{2+}]_{cyt}$. The type and duration of Ca^{2+} signals varied considerably between cell lines. Of utmost relevance is the question, whether the observed Ca^{2+} signals were specifically and genuinely mediated by TRPM8 channels.

Menthol is a non-specific TRPM8 agonist, yet has a significant preference for TRPM8; another cold receptor TRPA1 is stimulated by menthol only at millimolar concentrations in a heterologous expression system [41]. Moreover, the response to menthol (500 μM) is different in TRPM8-positive and TRPA1-positive neurons [42]. The same concentration (500 μM) had also been used in PC-3 cells to demonstrate the relevance of TRPM8 for menthol-induced Ca^{2+} responses [26]. In our experiments we did not find a positive correlation between total levels of TRPM8 expression and Ca^{2+} responses to menthol. This might be due in part to differences in the amount of functional TRPM8 channels in the plasma membrane and in ER compartments in the various cell lines.

Based on our experiments, only TRPM8 channels in the plasma membrane significantly contribute to Ca^{2+} responses. The involvement of TRPM8$_{ER}$ channels is likely minimal for the menthol-evoked Ca^{2+} signals We had previously reported similar results when comparing the contribution of TRPV1$_{ER}$ and TRPV1$_{PM}$ on capsaicin-evoked Ca^{2+} responses [17]. The poor responsiveness of LNCaP cells to menthol was rather surprising, given that LNCaP cell's TRPM8 protein expression levels were the highest of all investigated cell lines (Fig. 1A-B). Moreover, others have demonstrated Ca^{2+} responses in LNCaP cells after menthol administration [15]. Unlike in our study using Fluo-4 to measure $[Ca^{2+}]_{cyt}$, in the previous ones Fura-2 was used. Since Fura-2 and Fluo-4 have rather similar dissociation constants (K_d) for Ca^{2+} binding (200 nM *vs.* 345 nM, respectively), we consider it highly unlikely that the choice of Ca^{2+} indicator dye is the reason for the different results. The different experimental settings –trypsinized floating cells measured in a cuvette for the Fura-2 measurements [15] *vs.* analysis of attached single cells in our measurements – are the more likely reasons for the differences in the Ca^{2+} responses of LNCaP cells. We can however not entirely exclude that TRPM8 in LNCaP cells contain a subtle mutation (e.g. point mutation) rendering the protein non-functional. To definitively exclude off-target effects of menthol in the tested cells as reported before [38,43], we generated a TRPM8-knockout cell
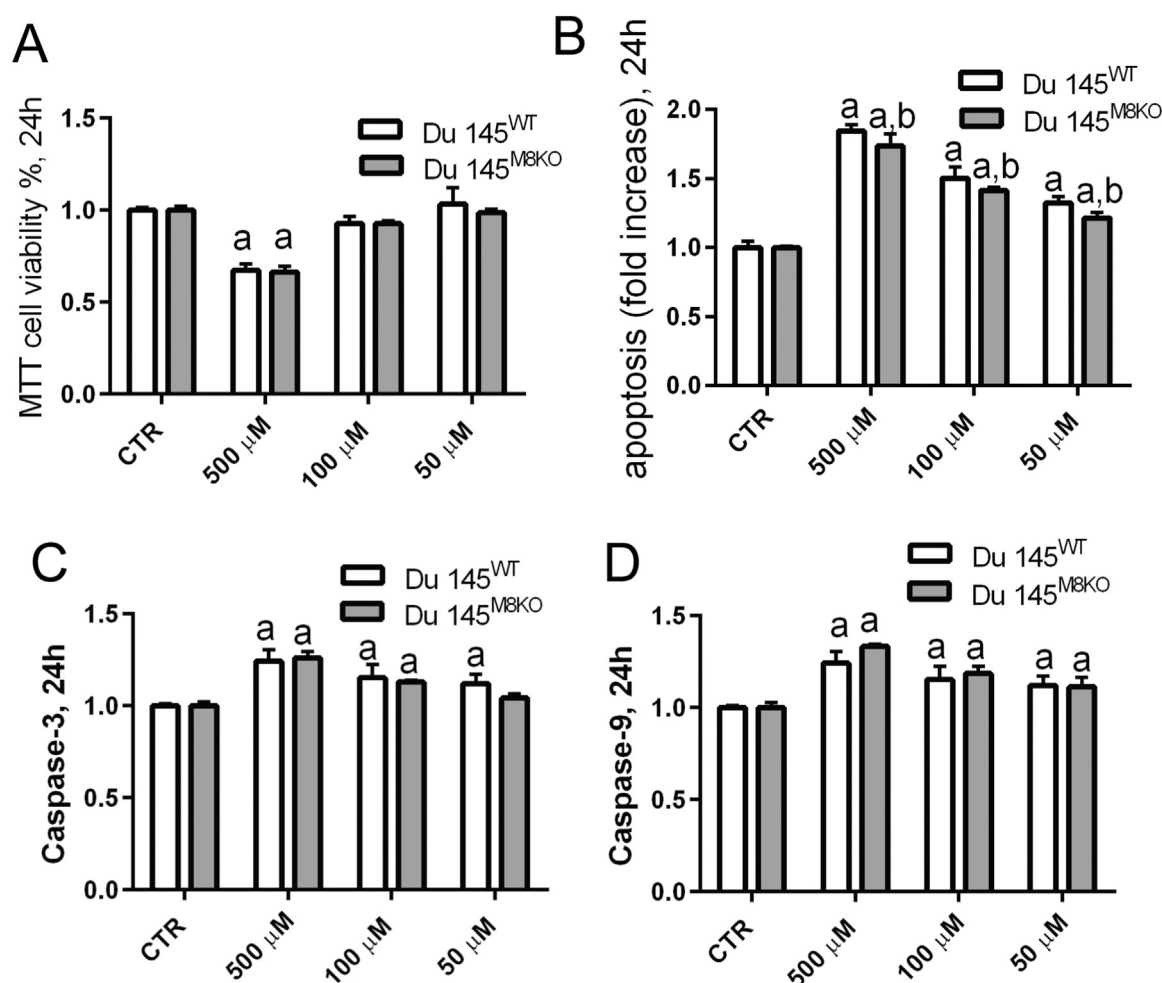
Fig. 5. Effects of menthol treatment on cell viability of Du 145^WT and Du 145^M8KO cells. A-D.) Cells were treated with menthol at different concentrations for 24 h. At this time point (24 h), MTT (**A**) and apoptosis assays were performed. Apoptosis was evidenced by loss of lipid asymmetry (**B**), caspase-3 (**C**) and capase-9 activities (**D**). The columns represent mean + standard deviation (SD) and n = 6 (2 independent experiments in triplicates). The letters on the columns denote the following: a - significant difference from control group, One-way ANOVA + post hoc Dunett test, b - significant difference between Du 145^WT and Du 145^M8KO cells at a given menthol concentration. One-way ANOVA + post hoc Sidak test.
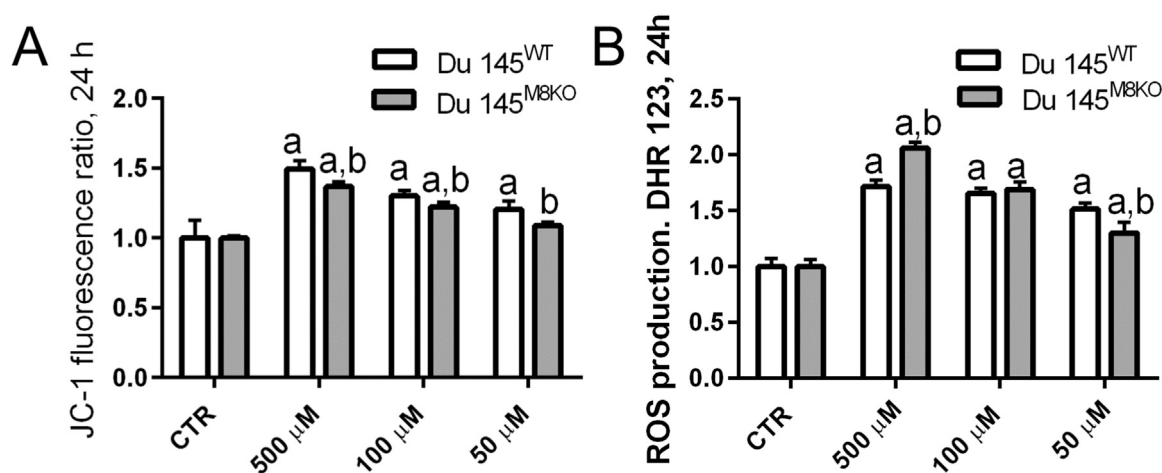
Fig. 6. Effects of menthol treatment on mitochondrial membrane depolarization and ROS production in Du 145^WT and Du 145^M8KO cells (mean + SD, n = 6, 2 independent experiments in triplicates). A-B) Cells were treated with menthol at different concentrations for 24 h. At this time point (24 h), cells were subjected to the JC-1 (**A**) and DHR 123 (**B**) assays indicating the levels of mitochondrial membrane potential and ROS production, respectively. The letters on the columns denote the following: a - significant difference from control group, p < 0.05, One-way ANOVA + post hoc Dunett test; b - significant difference between Du 145^WT and Du 145^M8KO cells at a given concentration of menthol; p < 0.05, one-way ANOVA + post-hoc Sidak test.
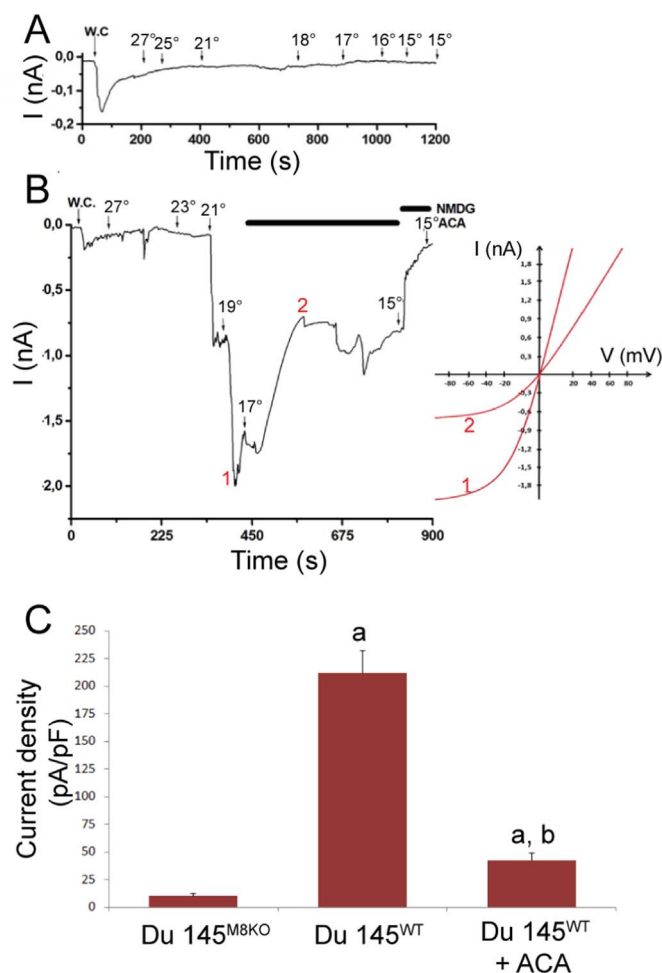
Fig. 7. Effects of cold on TRPM8 channel currents in Du 145 cells with and without TRPM8 (mean ± SD; n = 3 independent experiments). After whole-cell configuration (W.C.), the temperature of the patch chamber was gradually lowered from 27 °C to 15 °C by using a heat-controlled path-chamber and the currents were recorded in the patched cells. **A)** Recording from a Du 145^{M8KO} cell with cold stimulation. **B)** Recording from a Du 145^{WT} cell with cold stimulation and ACA inhibition. Corresponding I/V- relation (red traces) of currents recorded at the indicated time points 1 and 2. **C)** Current densities after cold exposure. Cold-evoked TRPM8 currents were blocked by extracellular ACA (0.025 mM). (^{a}p < 0.001 vs. the TRPM8 knockout group. ^{b}p < 0.001 vs. wild type without ACA treatment). (For interpretation of the references to color in this figure legend, the reader is referred to the web version of this article).

line derived from the highly menthol-responding cell line Du 145 (Du 145^{WT}) with the CRISPR/Cas9 technology. Since the generated Du 145^{M8KO} cells responded similarly to menthol as Du 145^{WT} cells in all assays, we conclude that the evoked Ca^{2+} signals leading to the evoked responses (impaired viability, mitochondria depolarization) are essentially independent of the presence of TRPM8 receptor.

The rhythmic increases in [Ca^{2+}]$_{cyt}$ after menthol stimulation are the result of an oscillating release of Ca^{2+} ions from the ER mediated by InsP$_3$ receptors, since blocking of the InsP$_3$-producing enzyme, phospholipase C by U-73122, resulted in a complete loss of Ca^{2+} oscillations (Fig. 3E). The activation of phospholipase C is either caused by an increase in [Ca^{2+}]$_{cyt}$ or by activation of G$_{\alpha q}$ proteins. Although an association between TRPM8 and G$_{\alpha q}$ proteins has been described before [44], there are several other plasma membrane receptors whose activation leads to the production of InsP$_3$ and Ca^{2+} oscillations. The human genome encodes approximately 750 G protein–coupled receptors, about 350 of which detect hormones, growth factors, and other endogenous ligands [45]. P2Y receptors are a family of purinergic G protein-coupled receptors sensitized by nucleotides such as ATP. P2Y receptors are present in almost all human tissues including tumors [46]

and moreover elevated concentration of extracellular ATP at the site of tissue injury or tumor mass were measured [47]. Extracellularly released ATP was found to play role in the spreading of Ca^{2+} waves between astrocytes [48] and other cell types [49]. Since the purinergic receptor blocker suramin and the presence of the ATP hydrolyzing enzyme apyrase in the extracellular milieu strongly diminished the menthol-evoked Ca^{2+} signals, we deduce that menthol induced an ATP release in tumor cells, however the identification of the precise mechanism remains elusive.

In biological systems many signaling pathways are tuned to sense stimulations in a certain physiological range; an over-stimulation often induces apoptotic processes. For instance, steroid receptor co-activators (SRC-1, SRC-2 and SRC-3) are involved in growth pathways required for tumor cell growth/proliferation, but potent SRC small molecule "stimulators" efficiently kill breast cancer cells by inducing aberrant cellular stress [50]. Prostate cancer rely on signals mediated via androgen receptors [51], but testosterone therapy for hypo-gonadal men with a history of prostate cancer lowers the recurrence of prostate cancer indicating that "overstimulation" of this signaling pathway also has beneficial anticancer effects [52]. In analogy, excess Ca^{2+} entry through plasma membrane Ca^{2+} channels induces apoptosis in many cell types [53]. A connection between excessive Ca^{2+} entry, mitochondrial Ca^{2+} accumulation and cytotoxic ROS production has also been documented in breast and prostate cancers. This, in turn, induces apoptotic processes [33,54], even if ROS production in a normal physiological range is important for growth of these cells [55]. Although menthol has antioxidant activity [56], in the current study, mitochondrial membrane depolarization, intracellular ROS production, apoptosis levels, and caspase-3 and -9 activities in Du 145 cells were increased in menthol-exposed prostate cancer cells. We hypothesize that this might be the result of an overstimulation of the purinergic pathway, but further studies are required to elucidate this question.

In conclusion, our study provided evidence that apoptotic pathways and mitochondrial ROS production through increased intracellular Ca^{2+} release were increased in Du 145 prostate cancer cells by 50–500 μM doses of menthol independently of the presence of TRPM8 channels. Moreover our data indicate that menthol affects purinergic signaling pathways.

Acknowledgements

Conflict of interest statement

The authors declare that they have no conflicts of interest with the contents of this article.

Authors' contributions

LP formulated the hypothesis, performed Ca^{2+} imaging and he was responsible for writing the report. MN and BÇ were responsible for the cell viability, apoptosis, caspase, ROS and JC-1 and electrophysiological analyses. WB, KJ, OZ performed PCR, cloning and Western blot, WB established the TRPM8 knockout cell line with the CRISPR/Cas9 method, TH performed the validation of the Du 145^{M8-KO} cells. KJ, CV, WB, TH, MN and BS contributed to writing and data analysis.

Appendix A. Supporting information

Supplementary data associated with this article can be found in the

online version at http://dx.doi.org/10.1016/j.redox.2017.10.009.

References

[1] T. Patel, Y. Ishiuji, G. Yosipovitch, Menthol: a refreshing look at this ancient compound, J. Am. Acad. Dermatol. 57 (2007) 873–878.

[2] J.A. Farco, O. Grundmann, Menthol – pharmacology of an important naturally medicinal "cool", Mini Rev. Med. Chem. 13 (2013) 124–131.

[3] G.P. Kamatou, I. Vermaak, A.M. Viljoen, B.M. Lawrence, Menthol: a simple monoterpene with remarkable biological properties, Phytochemistry 96 (2013) 15–25.

[4] C. Montell, The TRP superfamily of cation channels, Sci. STKE: Signal Transduct. Knowl. Environ. 2005 (2005) re3.

[5] C.L. Huang, The transient receptor potential superfamily of ion channels, J. Am. Soc. Nephrol. 15 (2004) 1690–1699.

[6] L. Tsavaler, M.H. Shapero, S. Morkowski, R. Laus, Trp-p8, a novel prostate-specific gene, is up-regulated in prostate cancer and other malignancies and shares high homology with transient receptor potential calcium channel proteins, Cancer Res. 61 (2001) 3760–3769.

[7] Z. Liu, H. Wu, Z. Wei, X. Wang, P. Shen, S. Wang, A. Wang, W. Chen, Y. Lu, TRPM8: a potential target for cancer treatment, J. Cancer Res. Clin. Oncol. 142 (2016) 1871–1881.

[8] N. Xiao, L.M. Jiang, B. Ge, T.Y. Zhang, X.K. Zhao, X. Zhou, Over-expression of TRPM8 is associated with poor prognosis in urothelial carcinoma of bladder, Tumour Biol.: J. Int. Soc. Oncodev. Biol. Med. 35 (2014) 11499–11504.

[9] N.S. Yee, Q. Li, A.A. Kazi, Z. Yang, A. Berg, R.K. Yee, Aberrantly over-expressed trpm8 channels in pancreatic adenocarcinoma: correlation with tumor size/stage and requirement for cancer cells invasion, Cells 3 (2014) 500–516.

[10] G. Bidaux, M. Flourakis, S. Thebault, A. Zholos, B. Beck, D. Gkika, M. Roudbaraki, J.L. Bonnal, B. Mauroy, Y. Shuba, R. Skryma, N. Prevarskaya, Prostate cell differentiation status determines transient receptor potential melastatin member 8 channel subcellular localization and function, J. Clin. Investig. 117 (2007) 1647–1657.

[11] A. Dhaka, T.J. Earley, J. Watson, A. Patapoutian, Visualizing cold spots: TRPM8-expressing sensory neurons and their projections, J. Neurosci. 28 (2008) 566–575.

[12] M.J. Berridge, The inositol trisphosphate/calcium signaling pathway in health and disease, Physiol. Rev. 96 (2016) 1261–1296.

[13] A.M. Dolmetsch, Nonlaser endoscopic endonasal dacryocystorhinostomy with adjunctive mitomycin C in nasolacrimal duct obstruction in adults, Ophthalmology 117 (2010) 1037–1040.

[14] T. Ishiguro, K. Ishikawa, M. Takahashi, M. Obayashi, T. Amino, N. Sato, M. Sakamoto, H. Fujigasaki, F. Tsuruta, R. Dolmetsch, T. Arai, H. Sasaki, K. Nagashima, T. Kato, M. Yamada, H. Takahashi, Y. Hashizume, H. Mizusawa, The carboxy-terminal fragment of alpha(1A) calcium channel preferentially aggregates in the cytoplasm of human spinocerebellar ataxia type 6 Purkinje cells, Acta Neuropathol. 119 (2010) 447–464.

[15] L. Zhang, G.J. Barritt, Evidence that TRPM8 is an androgen-dependent Ca2+ channel required for the survival of prostate cancer cells, Cancer Res. 64 (2004) 8365–8373.

[16] D. Chodon, A. Guilbert, I. Dhennin-Duthille, M. Gautier, M.S. Telliez, H. Sevestre, H. Ouadid-Ahidouch, Estrogen regulation of TRPM8 expression in breast cancer cells, BMC Cancer 10 (2010) 212.

[17] L. Pecze, W. Blum, T. Henzi, B. Schwaller, Endogenous TRPV1 stimulation leads to the activation of the inositol phospholipid pathway necessary for sustained Ca2+ oscillations, Biochim. Biophys. Acta 1863 (2016) 2905–2915.

[18] N. Rizaner, R. Onkal, S.P. Fraser, A. Pristera, K. Okuse, M.B. Djamgoz, Intracellular calcium oscillations in strongly metastatic human breast and prostate cancer cells: control by voltage-gated sodium channel activity, Eur. Biophys. J. 45 (2016) 735–748.

[19] P.A. Kosar, M. Naziroglu, I.S. Ovey, B. Cig, Synergic effects of doxorubicin and melatonin on apoptosis and mitochondrial oxidative stress in MCF-7 breast cancer cells: involvement of TRPV1 channels, J. Membr. Biol. 249 (2016) 129–140.

[20] M. Naziroglu, B. Cig, W. Blum, C. Vizler, A. Buhala, A. Marton, R. Katona, K. Josvay, B. Schwaller, Z. Olah, L. Pecze, Targeting breast cancer cells by MRS1477, a positive allosteric modulator of TRPV1 channels, PloS One 12 (2017) e0179590.

[21] G. Bidaux, A.S. Borowiec, D. Gordienko, B. Beck, G.G. Shapovalov, L. Lemonnier, M. Flourakis, M. Vandenberghe, C. Slomianny, E. Dewailly, P. Delcourt, E. Desruelles, A. Ritaine, R. Polakowska, J. Lesage, M. Chami, R. Skryma, N. Prevarskaya, Epidermal TRPM8 channel isoform controls the balance between keratinocyte proliferation and differentiation in a cold-dependent manner, Proc. Natl. Acad. Sci. USA 112 (2015) E3345–E3354.

[22] H.-U. Simon, A. Haj-Yehia, F. Levi-Schaffer, Role of reactive oxygen species (ROS) in apoptosis induction, Apoptosis 5 (2000) 415–418.

[23] A.C. Uguz, M. Naziroglu, J. Espino, I. Bejarano, D. Gonzalez, A.B. Rodriguez, J.A. Pariente, Selenium modulates oxidative stress-induced cell apoptosis in human myeloid HL-60 cells through regulation of calcium release and caspase-3 and -9 activities, J. Membr. Biol. 232 (2009) 15–23.

[24] E. Sakalli Cetin, M. Naziroglu, B. Cig, I.S. Ovey, P. Aslan Kosar, Selenium potentiates the anticancer effect of cisplatin against oxidative stress and calcium ion signaling-induced intracellular toxicity in MCF-7 breast cancer cells: involvement of the TRPV1 channel, J. Recept. Signal Transduct. Res. 37 (2017) 84–93.

[25] Z. Sun, H. Wang, J. Wang, L. Zhou, P. Yang, Chemical composition and anti-inflammatory, cytotoxic and antioxidant activities of essential oil from leaves of mentha piperita grown in China, PloS One 9 (2014) e114767.

[26] M.L. Valero, F. Mello de Queiroz, W. Stühmer, F. Viana, L.A. Pardo, TRPM8 ion channels differentially modulate proliferation and cell cycle distribution of normal and cancer prostate cells, PloS One 7 (2012) e51825.

[27] C.A. Whitlock, S.F. Ziegler, L.J. Treiman, J.I. Stafford, O.N. Witte, Differentiation of cloned populations of immature B cells after transformation with Abelson murine leukemia virus, Cell 32 (1983) 903–911.

[28] G. Tran Van Nhieu, B. Kai Liu, J. Zhang, F. Pierre, S. Prigent, P. Sansonetti, C. Erneux, J. Kuk Kim, P.G. Suh, G. Dupont, L. Combettes, Actin-based confinement of calcium responses during Shigella invasion, Nat. Commun. 4 (2013) 1567.

[29] L. Pecze, P. Pelsoczi, M. Kecskes, Z. Winter, A. Papp, K. Kaszas, T. Letoha, C. Vizler, Z. Olah, Resiniferatoxin mediated ablation of TRPV1 + neurons removes TRPA1 as well, Cana. J. Neurol. Sci 36 (2009) 234–241.

[30] P.R. de Jong, N. Takahashi, M. Peiris, S. Bertin, J. Lee, M.G. Gareau, A. Paniagua, A.R. Harris, D.S. Herdman, M. Corr, L.A. Blackshaw, E. Raz, TRPM8 on mucosal sensory nerves regulates colitogenic responses by innate immune cells via CGRP, Mucosal Immunol. 8 (2015) 491–504.

[31] L. Pecze, B. Schwaller, Characterization and modeling of Ca(2+) oscillations in mouse primary mesothelial cells, Biochim. Biophys. Acta 1854 (2015) 632–645.

[32] W. Blum, B. Schwaller, Calretinin is essential for mesothelioma cell growth/survival in vitro: a potential new target for malignant mesothelioma therapy? Int. J. Cancer 133 (2013) 2077–2088.

[33] B. Cig, M. Naziroglu, Investigation of the effects of distance from sources on apoptosis, oxidative stress and cytosolic calcium accumulation via TRPV1 channels induced by mobile phones and Wi-Fi in breast cancer cells, Biochim. Biophys. Acta 1848 (2015) 2756–2765.

[34] M. Naziroglu, C. Ozgul, Effects of antagonists and heat on TRPM8 channel currents in dorsal root ganglion neuron activated by nociceptive cold stress and menthol, Neurochem. Res. 37 (2012) 314–320.

[35] G. Nur, M. Nazıroğlu, H.A. Deveci, Synergic prooxidant, apoptotic and TRPV1 channelactivator effects of alpha-lipoic acid and cisplatin in MCF-7 breast cancer cells, J. Recept. Signal Transduct. Res. 37 (2017) 569–577.

[36] L. Pecze, W. Blum, B. Schwaller, Routes of Ca2+ shuttling during Ca2+ oscillations; focus on the role of mitochondrial Ca2+ handling and cytosolic Ca2+ buffers, J. Biol. Chem. (2015).

[37] E.S. Lashinger, M.S. Steiginga, J.P. Hieble, L.A. Leon, S.D. Gardner, R. Nagilla, E.A. Davenport, B.E. Hoffman, N.J. Laping, X. Su, AMTB, a TRPM8 channel blocker: evidence in rats for activity in overactive bladder and painful bladder syndrome, Am. J. Physiol. Ren. Physiol. 295 (2008) F803–F810.

[38] F. Mahieu, G. Owsianik, L. Verbert, A. Janssens, H. De Smedt, B. Nilius, T. Voets, TRPM8-independent menthol-induced Ca2+ release from endoplasmic reticulum and Golgi, J. Biol. Chem. 282 (2007) 3325–3336.

[39] L. Pecze, K. Josvay, W. Blum, G. Petrovics, C. Vizler, Z. Olah, B. Schwaller, Activation of endogenous TRPV1 fails to induce overstimulation-based cytotoxicity in breast and prostate cancer cells but not in pain-sensing neurons, Biochim. Biophys. Acta 1863 (2016) 2054–2064.

[40] J.J. Lemasters, T.P. Theruvath, Z. Zhong, A.L. Nieminen, Mitochondrial calcium and the permeability transition in cell death, Biochim. Biophys. Acta 1787 (2009) 1395–1401.

[41] M.A. Sherkheli, G. Gisselmann, H. Hatt, Supercooling agent icilin blocks a warmth-sensing ion channel TRPV3, Sci. World J. 2012 (2012) 982725.

[42] G.M. Story, A.M. Peier, A.J. Reeve, S.R. Eid, J. Mosbacher, T.R. Hricik, T.J. Earley, A.C. Hergarden, D.A. Andersson, S.W. Hwang, P. McIntyre, T. Jegla, S. Bevan, A. Patapoutian, ANKTM1, a TRP-like channel expressed in nociceptive neurons, is activated by cold temperatures, Cell 112 (2003) 819–829.

[43] S.H. Kim, J.H. Nam, E.J. Park, B.J. Kim, S.J. Kim, I. So, J.H. Jeon, Menthol regulates TRPM8-independent processes in PC-3 prostate cancer cells, Biochim. Biophys. Acta 1792 (2009) 33–38.

[44] X. Zhang, S. Mak, L. Li, A. Parra, B. Denlinger, C. Belmonte, P.A. McNaughton, Direct inhibition of the cold-activated TRPM8 ion channel by Galphaq, Nat. Cell Biol. 14 (2012) 851–858.

[45] D.K. Vassilatis, J.G. Hohmann, H. Zeng, F. Li, J.E. Ranchalis, M.T. Mortrud, A. Brown, S.S. Rodriguez, J.R. Weller, A.C. Wright, J.E. Bergmann, G.A. Gaitanaris, The G protein-coupled receptor repertoires of human and mouse, Proc. Natl. Acad. Sci. USA 100 (2003) 4903–4908.

[46] F. Di Virgilio, E. Adinolfi, Extracellular purines, purinergic receptors and tumor growth, Oncogene 36 (2017) 293–303.

[47] P. Pellegatti, L. Raffaghello, G. Bianchi, F. Piccardi, V. Pistoia, F. Di Virgilio, Increased level of extracellular ATP at tumor sites: in vivo imaging with plasma membrane luciferase, PloS One 3 (2008) e2599.

[48] E. Scemes, C. Giaume, Astrocyte calcium waves: what they are and what they do, Glia 54 (2006) 716–725.

[49] L. Leybaert, M.J. Sanderson, Intercellular Ca(2+) waves: mechanisms and function, Physiol. Rev. 92 (2012) 1359–1392.

[50] L. Wang, Y. Yu, D.C. Chow, F. Yan, C.C. Hsu, F. Stossi, M.A. Mancini, T. Palzkill, L. Liao, S. Zhou, J. Xu, D.M. Lonard, B.W. O'Malley, Characterization of a steroid receptor coactivator small molecule stimulator that overstimulates cancer cells and leads to cell stress and death, Cancer Cell 28 (2015) 240–252.

[51] E. Francini, M.E. Taplin, Prostate cancer: developing novel approaches to castration-sensitive disease, Cancer 123 (2017) 29–42.

[52] E.L. Rhoden, M.A. Averbeck, Testosterone therapy and prostate carcinoma, Curr. Urol. Rep. 10 (2009) 453–459.

[53] A. Verkhratsky, Calcium and cell death, Sub-Cell. Biochem. 45 (2007) 465–480.

[54] W.B. Zhu, F.J. Tian, L.Q. Liu, Chikusetsu (CHI) triggers mitochondria-regulated apoptosis in human prostate cancer via reactive oxygen species (ROS) production, Biomed. Pharmacother. = Biomed. Pharmacother. 90 (2017) 446–454.

[55] S.S. Brar, Z. Corbin, T.P. Kennedy, R. Hemendinger, L. Thornton, B. Bommarius, R.S. Arnold, A.R. Whorton, A.B. Sturrock, T.P. Huecksteadt, M.T. Quinn, K. Krenitsky, K.G. Ardie, J.D. Lambeth, J.R. Hoidal, NOX5 NAD(P)H oxidase regulates growth and apoptosis in DU 145 prostate cancer cells, American journal of physiology, Cell Physiol. 285 (2003) C353–C369.

[56] A.L. Rozza, F. Meira de Faria, A.R. Souza Brito, C.H. Pellizzon, The gastroprotective effect of menthol: involvement of anti-apoptotic, antioxidant and anti-inflammatory activities, PloS One 9 (2014) e86686.